Nanofabrication in cellulose acetate

Hongjun Zeng,* Robert Lajos, Vitali Metlushko, Ed Elzy, Se Young An and Joshua Sautner

Received 16th July 2008, Accepted 3rd November 2008
First published as an Advance Article on the web 26th November 2008
DOI: 10.1039/b812141a

We have demonstrated nanofabrication with commercialized cellulose acetate. Cellulose acetate is used for bulk nanofabrication and surface nanofabrication. In bulk nanofabrication, cellulose acetate reacts with an e-beam and permanent patterns are formed in it instead of being transferred to other substrates. We have studied the nano relief modulation performance of cellulose acetate before and after development. The depth of the nanopatterns is magnified after development, and is varied by exposing dosage and line width of the pattern. The thinnest 65 nm wide line is achieved in the bulk fabrication. We also demonstrate a binary phase Fresnel lens array which is directly patterned in a cellulose acetate sheet. Because of its unique mechanical and optical properties, cellulose is a good candidate for a template material for soft imprinting lithography. In the surface nanofabrication, cellulose acetate thin film spin-coated on silicon wafers is employed as a new resist for e-beam lithography. We achieved 50 nm lines with 100 nm pitches, dots 50 nm in diameter, and single lines with the smallest width of 20 nm. As a new resist of e-beam lithography, cellulose acetate has high resolution comparable with conventional resists, while having several advantages such as low cost, long stock time and less harmfulness to human health.

Introduction

Nanotechnology is increasingly regarded as an enabling tool in almost all fields of science and technology.[1] Especially, it promises to facilitate higher density circuits,[2] provide cleaner energy,[3,4] track and eliminate cancers,[5] *etc*. Nanofabrication is turning these promises into reality. In many cases, top-down nanofabrication or so-called nanomachining, employs similar processing concepts and schemes to those of microfabrication.[6] It includes part or all of the following steps: pattern generation, mask fabrication, resist preparation, pattern alignment and lithography, post exposure treatment and development, and pattern transfer (etching or imprinting), *etc*. The more steps a fabrication employs, the more time and hence cost will be spent, while more pattern transferring error will occur. Cutting down any of these steps but keeping comparable device performances is always desired in nanofabrication.

Herein we first report an approach to form nanopatterns in a bulk cellulose acetate (CA) sheet. The approach may directly lead to nano devices or master templates for imprinting lithography. CA in this research acts as both an e-beam sensitive material and a substrate material, therefore no resist coating and pattern transferring process are needed. Our research reveals that a CA sheet exposed to an e-beam has relief modulation capability before and after a development. We name the relief modulation before development as “real-time patterning”, and name the relief modulation after development as “direct patterning” since it does not need additional pattern transferring. Our experiments show that CA is capable of fabricating patterns on the order of tens of nanometers. On the other hand, we demonstrate that CA film spin-coated with its acetone solution can be an alternative to e-beam lithography (EBL) resists and is comparable to conventional ones[7–10] with high resolution, similar sensitivity, and good lift-off/dry etching performances. CA as well as its solvent and developer have significant advantages such as lower cost and less health harmfulness. In addition, without sensitizer and other additives, CA has much longer stock time than any other reported resists.

CA is one of the greatest inventions of the 20th century.[11] With many other important applications, it has been used widely as a substrate of motion picture and sheet film. In 1990s, Guo and co-workers used CA as a holographic material.[12,13] Holograms recorded in this material are very stable and can survive very high humidity.[14] Later it was reported that the material had the property of positive relief modulation which could lead to relief type of micro optical devices.[15,16] Since absorption of CA in most UV/visible ranges is very low,[17] in all of these researches it needed to be sensitized for UV light in ammonium dichromate and dimethyl sulfoxide solution. The related process is complicated, including sample soaking, post exposure baking, development delay, development, and soaking treatment in ethylidene lactic acid solution, however, the material's sensitivity is still low, and varied from a few hundred mJ cm^{-2} to several J cm^{-2}. The highest resolution is on the order of a few micrometers, which is not enough for nanolithography. In this paper, CA is employed for nanofabrication using e-beam lithography. Since e-beam possesses energy in the order of tens of thousands of electron volts (eV), much higher than UV light, falling in a range from a few to 100 eV, breaking bonds of CA molecules becomes much easier and more effective, without the requirement of any sensitizer and complicated treatment. Our work shows that CA can be used for either bulk or surface nanofabrication. The bulk nanofabrication is shown schematically in Fig. 1. Without any sensitizing process, resist spinning and pattern transferring,

Department of Electrical and Computer Engineering, University of Illinois at Chicago, 851 South Morgan Street, 1020 SEO, Chicago, Illinois, 60607. E-mail: hjzeng01@yahoo.com

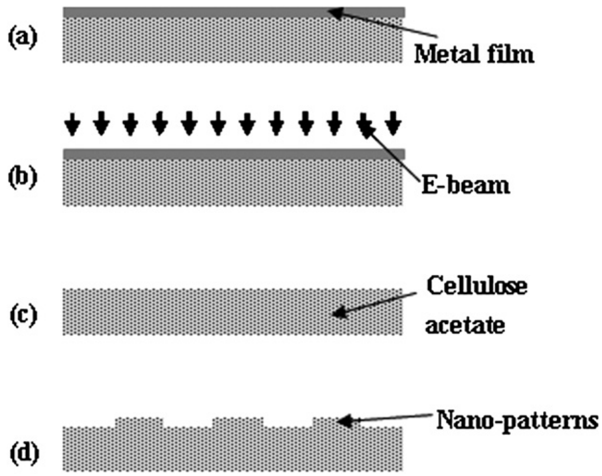

Fig. 1 Schematic of nanofabrication in CA. (a) Metal film coating on CA surface; (b) e-beam lithography; (c) wet etching metal film; and (d) development in NaOH solution.

a bulk nanofabrication with CA is much simpler than conventional methods. In the surface nanofabrication, CA is used as an e-beam resist and we demonstrate that it has very high resolution in standard nanofabrication processes such as lift-off or reactive ion etching (RIE).

Table 1 E-beam lithography parameters

Working distance	10 mm
Write field	100 μm^2
High voltage	10 kV
Aperture	30 μm
Beam current	220 pA
Area step size	20 nm
Line step size	10 nm
Area dose	100 μC cm^{-2}
Line dose	300 pC cm^{-1}
Isolated line dose (distance > 1 μm)	1000 pC cm^{-1}
Dot dose	0.1 pC

Real-time patterning

A commercialized CA sheet (McMaster Carr, Part#8564K55) for graphic applications, with 125 μm thickness is cut to 10 mm × 10 mm square pieces by scissors. Silver film with 12 nm thickness is then deposited on the CA squares by an electron beam evaporator. The deposition started in a vacuum of 5×10^{-7} T, with a deposition rate of 0.5 Å s^{-1}. The very thin metal film makes the CA surface conductive in order to eliminate the charge effect in the EBL step. The samples are subsequently exposed in a Raith E-Line EBL system, with all parameters listed in Table 1, and we define the dosage with these parameters as 100 percent of dose scale factor (DF), represented as DF 100, which means 100 μC cm^{-2} for area exposing, 300 pC cm^{-1} for line exposing and 0.1 pC for dot exposing. DF 50 means 50 percent of these dosages, *etc.*

Similar to the exposure under UV light,[15] CA has a strong real-time effect, *i.e.*, area exposed to the e-beam establishes height contrast with the unexposed area soon after the exposing. Fig. 2a shows the real-time depth of a 5 μm wide line measured by an atomic force microscope (Veeco Nanoscope III, contact mode, same below). At DF 12.5, the real-time depth is approximately 20 nm. The depth increases almost linearly before DF reaches 100. After that, the curve becomes flat and reaches a saturation depth at approximately 600 nm. We keep an exposed sample for a long enough time period, *i.e.* 2 months before we measured the depth again and found the depth increased averagely from 20 to 30% at all DFs. Although CA has similar real-time patterning after EBL as it is exposed to UV light, the mechanism is different from the previous reports which are based on a model where cellulose is cross-linked *via* Cr^{3+} provided by the sensitizer,[18] or a model where a gray level distribution is created by the color change of chromate in the cellulose.[16] Here we do not introduce any sensitizer, therefore the more reasonable explanation for the real-time patterning is: radiation of the e-beam directly decomposes the cellulose chains into shorter ones. Part of the byproducts resulting from the chain breaking may be gases which escape right away, and leave a real-time pattern; the other part byproducts may be smaller solid state molecules which stay at the original positions, but make the local area more soluble in the following development process.

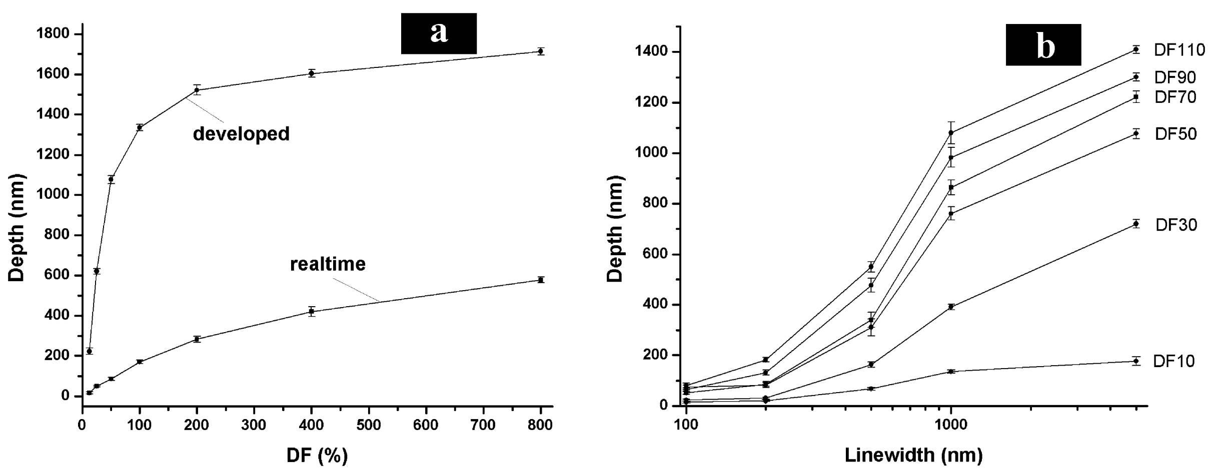

Fig. 2 Relief modulation performance of cellulose acetate. (a) Real-time and developed depth *vs.* dosage of a 5 μm wide line, and (b) developed depth *vs.* line width with different dosage. The depth of the lines is measured by contact mode AFM.

The real-time patterning provides a possibility of nanofabrication in CA with the shortest time. It can be used for fabrication of information recording devices such as computer generated holograms,[19] or other spatial modulators with low relief patterns. However, since the real-time depth is low and variable by time, its applications are limited.

Direct patterning in bulk CA

In the process of development, silver film is firstly etched away by a wet etchant (TFS-Transene Company, Inc.) at room temperature for 15 s followed by a 10 min deionized (DI) water rinse and blow drying with N_2, then the CA sample is soaked in a 3% (mass/volume) NaOH solution in DI water at room temperature for 1 min. The developing solution is agitated by magnetic stirring (60 rpm rotation speed). The sample is then rinsed by DI water for 15 min and blow dried by a N_2 gun. The depth of the developed patterns *vs.* DF value is also shown in Fig. 2a. By comparing the real-time depth and developed depth, we can see the depth of the nanopatterns is significantly magnified by the development. After DF goes beyond 100, the curve of the developed depth becomes flat and reaches a limit at approximately 1800 nm. By changing DF value, one can conveniently control the depth of relief in bulk CA, which provides opportunities to fabricate 3-D structures and devices on a chip.

Fig. 2b shows a relationship between the developed depth and line width, *i.e.*, spatial frequency response with different dosage. All curves indicate that the depth of the lines increases when line width increases, with an inflection point at width 1000 nm. Wide lines achieve much larger depth at higher dosages than they do at lower dosages, but the depth of the narrower lines is more independent with dosage. The radius of the AFM tip we used is approximately 40 nm, therefore we could not measure the depth if the line width is less than 100 nm.

We observed the proximity effect in the e-beam lithography.[20] Fig. 3 shows a typical cross sectional profile of lines with widths under investigation. We found in our experiment, 200 nm wide lines with 400 nm pitches suffered the most from the proximate effect because the lines have the largest height difference from their top to the unexposed area. Comparing this difference among all dose factors in Table 2, we can see the proximate effect increases as the dose factor goes up. How to depress or even eliminate the proximity effect is one of the goals in our next step of research.

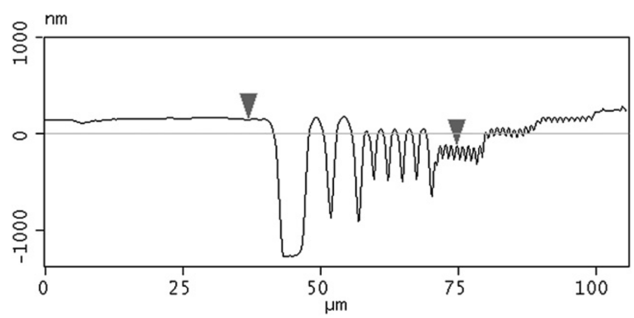

Fig. 3 Cross sectional profile of nano lines in CA with different width and period. The left flat profile is the unexposed area. The profile is scanned by a contact AFM.

Table 2 Height difference between top of 200 nm lines and unexposed area

DF	Height difference/nm
10	48.6
30	88.3
50	168.7
70	220.6
90	248.9
110	271.5

Although the proximity effect has not been depressed, we are still able to demonstrate that bulk CA sheet has high resolution. Fig. 4a contains isolated pixel lines with a spacing of 2 μm and a DF from 100 to 450 in steps of 10. As the dosage increases, the line width and depth becomes larger. Fig. 4b shows a zoom-in image of the finest lines with a width of 65 nm and a depth of 40 nm. Again because the radius of the AFM tip is about 40 nm, the real depth should be larger than the measured value. With so high resolution, we could "direct pattern" complicated nanostructures in CA. Since CA has relatively high mechanical strength, excellent optical clarity, and a high dielectric constant, such a "direct patterning" capability provides the opportunity of quickly fabricating nano devices for applications in optics, electronics and micro/nano fluidics.

To demonstrate that functional devices can be directly fabricated from CA, we have fabricated a 4 × 4 array of binary phase Fresnel lens (Fig. 5a). Fig. 5b shows the details of one lenslet scanned by an AFM, with a 50 μm diameter, and 250 nm smallest zone width. If we put an object (characters "UIC" in this case) in front of the array, we are able to capture its image generated by the array with a microscope, shown in Fig. 5c and 5d, which demonstrates the capability of the CA lens array as an optical imaging device. The roughness of the device at the patterned and unpatterned area is measured as 8.2 nm and 8.7 nm, respectively (arithmetic average from measurements on five 5 μm × 5 μm squares for each case). This means the nanofabrication does not increase the surface roughness, which is important for many applications such as those in optics. As a contrast, the roughness of a device usually increases after the pattern transfer *via* RIE, especially if the transferred depth is large.

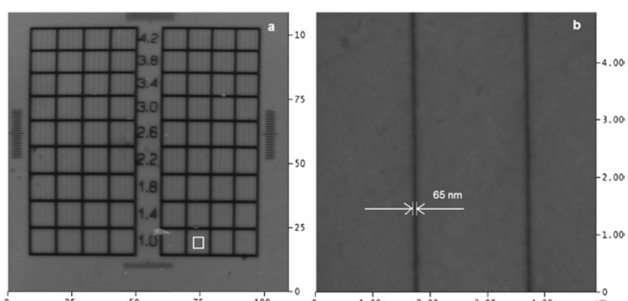

Fig. 4 AFM images of isolated lines in CA with DF from 100 to 450 after development. (a) Overview of lines. The numbers in the middle are the magnitudes of dosage, 1.0 = DF 100; and (b) the finest lines magnified from the white square in (a). The period of the lines is 2 μm.

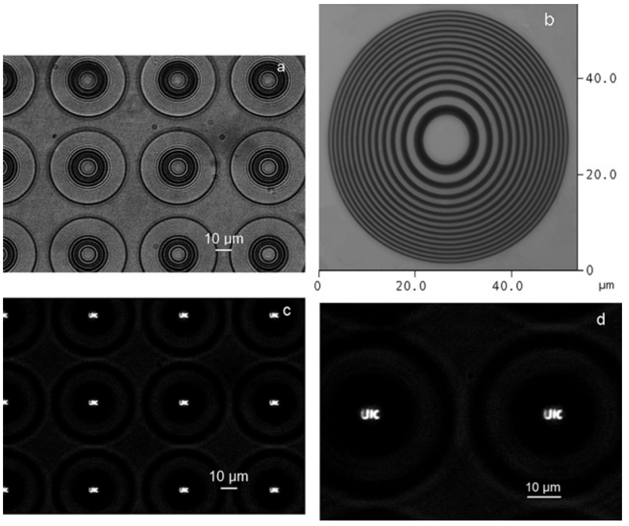

Fig. 5 Binary phase Fresnel lens array in CA after development. (a) Micrograph of the lens array; (b) AFM image of one lenslet with geometrical details; (c) micrograph of image generated by the lens array; and (d) magnified micrograph of the image. The object is illuminated by a halogen lamp.

In soft imprinting lithography,[21] nanopatterns need to be transferred into a bulk material of a master template so that they can survive the repetitive press and release process. Now we see that nanopatterns are able to be fabricated directly in a bulk CA sheet, a good candidate to greatly simplify the process of imprint lithography. The elastic modulus of CA is ~500 N mm^{-2}, much higher than that of poly(dimethylsiloxane) (PDMS), a most commonly used template material in soft imprinting lithography, typically with a modulus of several N mm^{-2}.[22] A high modulus is a key factor in providing opportunities for transferring high resolution patterns. Good flexibility of the CA sheet decreases the possibility of cracking the master template or damaging small features, and it is desirable for the roll-to-roll imprinting technique.[23] For UV light with wavelength larger than 360 nm, the transmittance of CA > 80%.[17] The softening point of CA is higher than 260 °C (cellulose triacetate can be even higher). These properties provide CA with the feasibility to be a master template material for both UV radiation and thermal imprinting. Investigation of imprinting lithography with a CA master template is out of the scope of this paper but will be reported in another paper.

Surface nanofabrication with CA as an EBL resist

Our research shows that CA is not only a "direct patterning" material, but also a resist material for nanofabrication with performances comparable to poly(methyl methacrylate) (PMMA), one of the most commonly used EBL resists. We dissolved CA in acetone and achieved a CA–acetone solution with a concentration of 2% (mass/volume). Currently there is no CA specifically for nanofabrication, therefore we used commercialized graphic CA sheets. They contain many particles, so we removed most particles larger than 0.1 μm by a filter. Silicon wafers are first cleaned by Piranha and buffered oxide etchants. Hexamethyldisilazane (HMDS) is then applied on the silicon wafers to enable better film adhesion and smoothness. The CA solution is then spun on the silicon wafers by a photoresist spinner (Headway, model#PWM101), with a speed of 3500 rpm for 30 s, followed by prebaking on a hot plate at 170 °C for 10 min. A bake temperature at 170 °C gives CA film a strong adhesion to the silicon substrate, while temperatures below 120 °C leads to an ease of peeling off from the substrate in or after development. The film is measured to be 60 nm in thickness and 6.7 nm in roughness in a 5 μm × 5 μm area.

Using the same conditions provided in Table 1 the e-beam lithography is performed in the CA thin film. It is interesting that we did not see any real-time pattern after the exposing and currently do not have a proper explanation about it. Nanopatterns in CA are achieved after a development in a 3% NaOH solution in DI water at room temperature for 1 min. The developing solution is agitated by magnetic stirring (60 rpm rotation speed). The sample is then rinsed by DI water for 15 min and blow dried by a N_2 gun. The patterns are coated by Cr/Cu with thickness of 5 nm/12 nm in the e-beam thermal evaporator. We then soak the samples in acetone for 10 min and subsequently perform an ultrasonic clean for 3 min. The resulting metal patterns are inspected by SEM. In Fig. 6a, a SEM image shows periodical lines with a 50 nm width and a 100 nm pitch. The narrowest single line we achieved is 20 nm wide, shown in Fig. 6b. With so narrow Cr/Cu lines as templates, we may be able to fabricate extremely small nanochannels *via* the fast galvanic sacrificial method.[24] Fig. 6c shows a dot array, which is 50 nm in diameter and 500 nm in pitch. All these images demonstrate that the lithographic resolution of CA is as high as that of PMMA. Especially, the width of the single line in Fig. 6b has reached the line width limit of the E-Line EBL system under the same conditions. If a higher voltage of the e-beam is used, *i.e.* > 50 kV, a line width smaller than 20 nm may be expected.

We also tried to transfer the nanopatterns from CA resist to silicon substrate by a RIE system (STS 310), with 40 sccm SF_6, 80 W RF power and 30 mT. The etching time is 10 s. The etching selectivity between CA and Si is measured approximately as 1 : 0.9. Fig. 7 shows the patterns transferred in the silicon substrate. As Fig. 7a shows, the 50 nm-width, 100 nm-pitch lines were

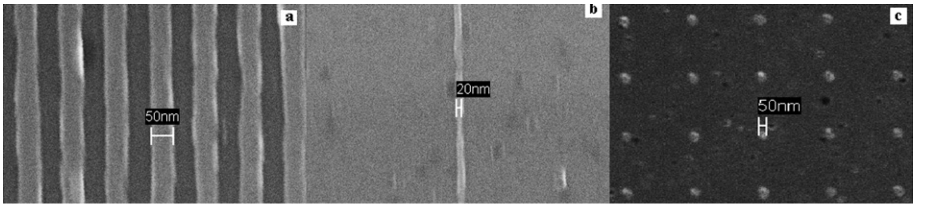

Fig. 6 SEM images of Cr/Cu nanopatterns from lift-off. (a) 50 nm lines with 100 nm pitches; (b) 20 nm single line; and (c) 50 nm dots array with 500 nm pitches. SEM voltage = 10 kV, aperture = 30 μm.

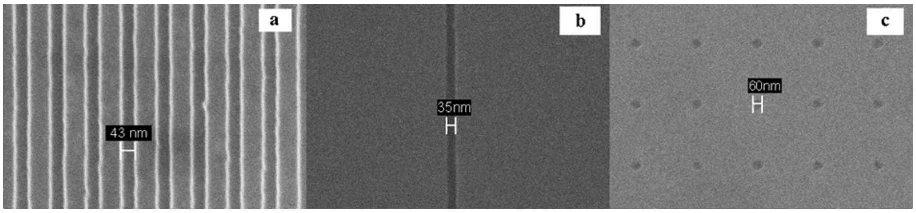

Fig. 7 SEM images of silicon nanopatterns after RIE transfer. (a) ~45 nm lines with 100 nm pitches; (b) 35 nm single line; and (c) 60 nm dots array with 500 nm pitches. SEM voltage = 10 kV, aperture = 30 μm.

transferred with the line width slightly decreased to approximately 45 nm. The finest single line transferred in silicon is 35 nm, shown in Fig. 7b and the smallest dots are 60 nm in diameter in Fig. 7c. The average roughness of the etched area is measured as 10.3 nm in a 5 μm × 5 μm area.

CA is made from renewable resources such as wood pulp or cotton linters which go through a process of hydrolysis and precipitation with glacial acetic acid and catalyst.[11] Introducing e-beam as a radiation source not only enables the nanolithography in CA, but avoids using toxic chemicals such as chromate. In surface nanofabrication, CA employs acetone as the solvent, which is less hazardous than the solvents of PMMA such as anisole or chlorobenzene. Without the sensitizer, dark reaction[16] is completely eliminated and so CA's stock time can be extremely long until degradation (known as "vinegar syndrome") occurs. Actually, CA can be stored for about 100 years in a clean room environment with 60 °F temperature and 40% relative humidity,[25] which is much longer than any conventional resist, *e.g.*, PMMA 950 C5 EBL resist (Microchem, Inc.) whose stock life is only 1 year.

Conclusion

We have reported using CA for nanofabrication. CA is not only an e-beam sensitive material but also a substrate material with high flexibility, high elastic modulus, relative low UV absorption, and high softening point, which enable CA to be a good candidate for a "direct patterning" material for fabricating nano devices or imprinting templates. We also demonstrate that CA can be a new e-beam resist, with high resolution and capability of nanomachining for lift-off and RIE pattern transferring. Note that the exposing conditions in Table 1 are designed for PMMA, we know the exposing sensitivity of CA is also close to that of PMMA. CA itself is a renewable material with a very long stock time, and its related nanofabrication is significantly simpler, cheaper, more biocompatible and less harmful for the human's health. Our future work of the CA based nanofabrication includes eliminating the proximate effect and developing an imprinting lithography technique with CA as the template material.

Acknowledgements

All fabrication and characterization of this paper is done in the Nanotechnology Core Facility, University of Illinois at Chicago. The pattern file in the e-beam lithography is provided by RaithUSA, Inc. The authors would like to thank Mrs Meiling Yan and Mr Qixing Tao for their great support and help.

References

1 *The National Nanotechnology Initiative at Five Years: Assessment and Recommendations of the National Nanotechnology Advisory Panel*, May 2005, available on-line at http://www.nano.gov/FINAL_PCAST_NANO_REPORT.pdf.
2 M. Forshaw1, R. Stadler, D. Crawley and K. Nikoli'c, *Nanotechnology*, 2004, **15**, S220–S223.
3 J. Y. Lee, K. H. An, J. K. Heo and Y. H. Lee, *J. Phys. Chem. B*, 2003, **107**, 8812–8815.
4 W. Ma, C. Yang, X. Gong, K. Lee and A. J. Heeger, *Adv. Funct. Mater.*, 2005, **15**, 1617–1622.
5 M. Ferrari, *Nature*, 2003, **5**, 161–171.
6 M. J. Madou, *Fundamentals of Microfabrication: The Science of Miniaturization*, CRC Press, ISBN: 0849308267, 2002.
7 L. E. Ocola, M. I. Blakey, P. A. Orphanos, W. Y. Li, R. J. Kasica and A. E. Novembre, *J. Photopolymer Sci. and Technol.*, 2001, **14**, 547–554.
8 M. Hatzakis, *J. Electrochem. Sco.: Electorchemical Technology*, 1969, **116**, 1033–1037.
9 B. Bilenberg, S. Jacobsen, M. S. Schmidt, L. H. D. Skjolding, P. Shi, P. Bøggild, J. O. Tegenfeldt and A. Kristensen, *Microelectron. Eng.*, 2006, **83**, 1609–1612.
10 L. An, Y. Zheng, K. Li, P. Luo and Y. Wu, *J. Vac. Sci. Technol., B*, 2005, **23**, 1603–1606.
11 P. J. T. Morris, *The American Synthetic Rubber Research Program*, University of Pennsylvania Press, ISBN 0-8122-8207-8, 1989.
12 L. R. Guo, Q. R. Chen and K. P. Wang, *Proc. SPIE*, 1991, **1461**, 91–92.
13 K. Wang, L. Guo, Q. Chen, C. Dai, J. Zhu and P. Xu, *Opt. Lett.*, 1994, **19**, 1240–1242.
14 Q. R. Chen, G. P. Wang, L. R. Guo and C. M. Dai, *Sci. China Series A*, 1994, **37**, 108–112.
15 J. Zhu, H. Zeng and L. Guo, *Proc. SPIE*, 1996, **2866**, 405–407.
16 J. Zhu, K. Wang, L. Guo, Q. Huang and Y. Guo, *Appl. Opt.*, 1998, **37**, 4330–4336.
17 A. K. SHARMA and C. H. RAMU, *J. Mater. Sci. Lett.*, 1991, **10**, 1217–1219.
18 K. Wang, L. Guo, L. Zhou and J. Zhu, *Appl. Opt.*, 1996, **35**, 6369–6374.
19 B. R. Brown and A. W. Lohmann, *Appl. Opt.*, 1966, **5**, 967–969.
20 E. Kratschmer, *J. Vac. Sci. Technol*, 1981, **19**, 1264–1268.
21 T. W. Odom, J. C. Love, D. B. Wolfe, K. E. Paul and G. M. Whitesides, *Langmuir*, 2002, **18**, 5314–5320.
22 M. Bender, U. Plachetka, J. Ran, A. Fuchs, B. Vratzov, H. Kurz, T. Glinsner and F. Lindner, *J. Vac. Sci. Technol., B*, 2004, **22**, 3229–3232.
23 T. Mäkelä, T. Haatainen, P. Majander and J. Ahopelto, *Microelectron. Eng.*, 2007, **84**, 877–879.
24 H. Zeng, Z. Wan and A. D. Feinerman, *Nanotechnology*, 2006, **17**, 3183–3188.
25 J. M. Reilly, *IPI Guide for Acetate Film*, Image Permanence Institute, Rochester, NY, 1993. Available on-line at http://www.imagepermanenceinstitute.org/shtml_sub/acetguid.pdf.